

# Helional induces Ca<sup>2+</sup> decrease and serotonin secretion of QGP-1 cells via a PKG-mediated pathway

Benjamin Kalbe<sup>1</sup>, Marian Schlimm<sup>1</sup>, Julia Mohrhardt<sup>2</sup>, Paul Scholz<sup>1</sup>, Fabian Jansen<sup>1</sup>, Hanns Hatt<sup>1</sup> and Sabrina Osterloh<sup>1</sup>

<sup>1</sup>Department of Cell Physiology, Ruhr-University Bochum, Bochum, Germany

<sup>2</sup>Department of Chemosensation, Institute for Biology II, RWTH Aachen University, Aachen, Germany

Correspondence  
should be addressed  
to B Kalbe

**Email**  
benjamin.kalbe@rub.de

## Abstract

The secretion, motility and transport by intestinal tissues are regulated among others by specialized neuroendocrine cells, the so-called enterochromaffin (EC) cells. These cells detect different luminal stimuli, such as mechanical stimuli, fatty acids, glucose and distinct chemosensory substances. The EC cells react to the changes in their environment through the release of transmitter molecules, most importantly serotonin, to mediate the corresponding physiological response. However, little is known about the molecular targets of the chemical stimuli delivered from consumed food, spices and cosmetics within EC cells. In this study, we evaluated the expression of the olfactory receptor (OR) 2J3 in the human pancreatic EC cell line QGP-1 at the mRNA and protein levels. Using ratiofluorometric Ca<sup>2+</sup> imaging experiments, we demonstrated that the OR2J3-specific agonist helional induces a transient dose-dependent decrease in the intracellular Ca<sup>2+</sup> levels. This Ca<sup>2+</sup> decrease is mediated by protein kinase G (PKG) on the basis that the specific pharmacological inhibition of PKG with Rp-8-pCPT-cGMPs abolished the helional-induced Ca<sup>2+</sup> response. Furthermore, stimulation of QGP-1 cells with helional caused a dose-dependent release of serotonin that was comparable with the release induced by the application of a direct PKG activator (8-bromo-cGMP). Taken together, our results demonstrate that luminal odorants can be detected by specific ORs in QGP-1 cells and thus cause the directed release of serotonin and a PKG-dependent decrease in intracellular Ca<sup>2+</sup>.

## Key Words

- ▶ olfactory receptor
- ▶ serotonin
- ▶ enterochromaffin cells
- ▶ calcium signaling

*Journal of Molecular  
Endocrinology*  
(2016) **57**, 201–210

## Introduction

Enterochromaffin (EC) cells, the most abundant endocrine cell type, regulate the important functions of the gut, stomach, gall bladder, intestine and pancreas by secreting biologically active signaling molecules (e.g. gastrin, chromogranins, secretin, somatostatin and cholecystokinin) that are synthesized and stored within these cells (Moran *et al.* 2008, Manocha & Khan 2012). One of the most prominent transmitters is serotonin (5-hydroxytryptamine, 5-HT), which controls among others epithelial transport,

peristalsis, inflammatory processes, osteogenesis and the transmission to afferent neurons, and peristalsis is also critically dependent on the activation of serotonergic neurons (Gershon 2004, 2013, Li *et al.* 2011, Heredia *et al.* 2013). In general, the release of serotonin is mediated by an increase of the intracellular Ca<sup>2+</sup> concentration via influx of extracellular Ca<sup>2+</sup> or liberation from intracellular stores and exocytosis of vesicles (Racké *et al.* 1996). Cyclic adenosine monophosphate (cAMP) can also lead to the

release of serotonin after mechanical stimulation or stimulation with odorants (Braun *et al.* 2007, Chin *et al.* 2012). Serotonin receptors are often used as therapeutic targets for the treatment of EC cell-associated diseases, such as irritable bowel syndrome (Bischoff *et al.* 2014). Therefore, the characterization of EC cells is important to understand the physiology of the gastrointestinal tract. Although human EC cells are difficult to investigate because they constitute a small subpopulation within a given tissue, several cell lines, including KRJ-1, BON or QGP-1 cells, have been established that mimic the EC features (Pfragner *et al.* 2009, Siddique *et al.* 2009). A few studies have shown that EC cells can act as specialized chemosensors by detecting distinct odorants (BON cells) (Braun *et al.* 2007), pungent irritants (QGP-1 cells) (Doihara *et al.* 2009) or bitter stimuli (STC-1 cells) (Wu *et al.* 2002) through olfactory receptors (ORs), transient receptor potential (TRP) channels or taste receptors, respectively.

In recent years, emerging studies have demonstrated that OR expression can be found in various human cell types in addition to the olfactory tissues (Feldmesser *et al.* 2006, Flegel *et al.* 2013). These receptors are functionally expressed in muscle cells (Pavlath 2010), keratinocytes (Busse *et al.* 2014) and sperm cells (Spehr *et al.* 2003) as well as in prostate cancer cells (Neuhaus *et al.* 2009), leukemia cells (Manteniotis *et al.* 2016), the EC cell line BON (Braun *et al.* 2007) and hepatocarcinoma cells (Maßberg *et al.* 2015), in which they regulate important physiological processes, such as proliferation or migration. ORs constitute a supergene family within the class of G protein-coupled receptors (GPCRs) and are activated by specific odorants. In the olfactory sensory neurons (OSNs), a conformational change of the OR is initialized, which triggers a cAMP-dependent signal transduction cascade and opening of cyclic nucleotide-gated (CNG) channels. However, in addition to the canonical olfactory pathway, various alternative signaling components have been described. It has been shown that alternative G proteins (others than G<sub>olf</sub>) can be activated, which lead to an inhibition of the classical odor response (Spehr *et al.* 2002, Ache 2010). Additionally, diverse downstream signaling molecules, including Src kinase and mitogen-activated protein kinases (MAPK), can be involved in ectopic OR signaling (Neuhaus *et al.* 2009, Spehr *et al.* 2011, Maßberg *et al.* 2015).

In this study, we evaluated the RNA and protein levels of specific ORs in the human pancreatic EC cell line QGP-1. The application of the odorant helional led to dose-dependent decreases in intracellular Ca<sup>2+</sup> levels. The inhibition of PKG through a specific blocker caused a significant suppression of the observed effect.

Additionally, OR2J3 stimulation with helional induced a dose-dependent release of serotonin from the QGP-1 cells.

## Materials and methods

### Culture of the QGP-1 cells

The QGP-1 cells were the kind gift of Prof. Dr Massimo Donadelli (University of Verona, Italy). They were cultured in RPMI-1640 medium with 10% fetal bovine serum (FBS) and 100 U/mL penicillin and streptomycin at 37°C in a 5% CO<sub>2</sub> humidified atmosphere as described elsewhere (Iguchi *et al.* 1990). Gibco supplements and media were purchased from Thermo Fisher Scientific if not otherwise indicated.

### Total RNA isolation and reverse transcriptase-PCR

Total RNA was extracted from the QGP-1 cells using an RNeasy Mini Kit (Qiagen) according to the manufacturer's instructions. The RNA concentration and quality (A260/A280 ratio) were analyzed using a NanoDrop ND-1000 Spectrophotometer (Thermo Scientific). After DNase I treatment with a TURBO DNA-free Kit (Thermo Scientific), complementary DNA (cDNA) was synthesized using an iScript cDNA Synthesis Kit (Bio-Rad). For the reverse transcriptase (RT)-PCR experiments, we included RNA-only controls (-RT) to exclude genomic DNA (gDNA) contamination. RT-PCR was performed using the GoTaq qPCR Master Mix (Promega) in a volume of 20 µL with 10 pmols of each primer. The following temperature cycle profile was used to detect β-actin, OR2J3, OR3A1 and OR1A2: 5 min at 95°C followed by 40 cycles of 45 s at 95°C, 45 s at 60°C, 45 s at 72°C and a final extension of 10 min at 72°C. The following primers were used: β-actin (forward: 5'-GTACCCAGGCATTGCTGACA-3', reverse: 5'-AGAAAGGGTGTAAAACGCAGC-3'), OR2J3 (forward: 5'-TGCTAGCTCTGAGGGTACTT-3', reverse: 5'-AGAGATGGTCTTTTCCGGGC-3'), OR3A1 (forward: 5'-TTCGCTCTGTAGAGGGCAGG-3', reverse: 5'-TGAGCATCCTCCAGATGGCA-3'), OR1A2 (forward: 5'-CTGGGTCTTGGGTGATTGGAA-3', reverse: 5'-GGTGCAGAAGGCTTTGAATAGAC-3'). As a positive control for the primers, human gDNA was used. The resulting primer products were confirmed using Sanger sequencing.

### Immunocytochemical staining

The QGP-1 cells were cultured on 30-mm coverslips until they were 80% confluent. After a washing step using PBS, the cells were fixed with ice-cold acetone for 5 min. To

avoid nonspecific antibody binding, the cells were blocked in 1% cold-water fish gelatin (Sigma-Aldrich) diluted in TBS with 0.05% Triton X-100 (Sigma-Aldrich), followed by incubation with the primary antibody. A primary antibody directed against OR2J3 (rabbit polyclonal) (SAB4501918, Sigma-Aldrich) was used. The cells were co-incubated with 4'-6-diamidin-2-phenylindol (DAPI) fluorescent dye to label the nuclei. The fluorophore-coupled secondary antibodies Alexa Fluor 488 nm (goat anti-rabbit) (#A-11034, Thermo Fisher Scientific) and 546 nm (goat anti-rabbit) (#A-11010, Thermo Fisher Scientific) were used, and cells were coated with ProLong Antifade Gold (Thermo Fisher Scientific). The fluorescent signals were detected using confocal microscopy (Zeiss LSM 510 Meta, Oberkochen, Germany) with a 40× oil immersion objective and the Leica Application Suite software (LAS, Leica). The images were processed using Corel Draw X5 (Corel, Ottawa, ON, Canada).

### Western blotting

A lysate of the total cellular proteins was extracted in an appropriate volume of RIPA buffer after sedimentation of the QGP-1 cells. The extract was then mechanically homogenized and centrifuged (1000g for 10 min at 4°C). A sample of the whole protein fraction was collected and prepared in Laemmli's buffer for Western blot analysis, which was performed as described elsewhere (Neuhaus *et al.* 2009). The samples were loaded onto sodium dodecyl sulfate (SDS) gels and blotted to nitrocellulose membranes. After a blocking step in 50% casein (50% TBS buffer and 50% casein in TBS, Thermo Scientific), the membranes were incubated with primary antibody diluted in 75% TBS buffer and 25% casein. For immunodetection, a horseradish peroxidase (HRP)-coupled secondary antibody (goat anti-rabbit) (#170-6515, Bio-Rad) was used. The chemiluminescence was imaged using Fusion-SL 3500-WL (Vilber Lourmat, Eberhardzell, Germany). The OR2J3 antibody (rabbit, polyclonal, 1:250) was purchased from Sigma-Aldrich (SAB4501918). As a protein loading control,  $\beta$ -actin antibody (rabbit polyclonal, 1:1000) was used (ab8227, Abcam).

### Calcium imaging

The QGP-1 cells were cultured in 35-mm cell culture dishes (Sarstedt, Nümbrecht, Germany). After reaching approximately 80% confluence, the cells were incubated with 3  $\mu$ M fura-2-acetoxymethyl ester (Molecular Probes,

Thermo Fisher Scientific) for 30 min at 37°C. The growth medium was replaced with an extracellular Ringer's solution, and fluorometric imaging was performed as described previously (Neuhaus *et al.* 2009). The cells were exposed to the relevant substances according to the experimental approach using a specialized microcapillary application system. All the substances were prediluted in DMSO (maximal final concentration of 0.1%) and dissolved in the extracellular solution to the desired concentration. All odorants and odorant mixtures, as well as allyl isothiocyanate (AITC) and the PKG activator 8-bromo-cGMP were directly applied for 60s. The cells were preincubated with the PKG-specific inhibitor Rp-8-pCPT-cGMPS (30  $\mu$ M) for 6 min. AITC was purchased from Sigma-Aldrich. 8-Bromo-cGMP and Rp-8-pCPT-cGMPS were obtained from Enzo Life Sciences (Farmingdale, NY, USA). As a negative control, DMSO (0.1%) was used in Ca<sup>2+</sup> imaging experiments.

### Odorants

The odorants were divided into four different mixtures (containing various odorants (each at 300  $\mu$ M) that are known to be ligands for specific deorphanized ORs) according to their chemical structures. Odorant mixture 1 (OM1):  $\beta$ -ionone (OR51E2 (Neuhaus *et al.* 2009)), bourgeonal (OR1D2 (Spehr *et al.* 2003)), helional (OR3A1 (Wetzel *et al.* 1999), OR1A1 and OR1A2 (Schmiedeberg *et al.* 2007) and OR2J3 (Adipietro *et al.* 2012)); odorant mixture 2 (OM2): amyl butyrate (OR2AG1 (Neuhaus *et al.* 2006)), methyl octanoate (OR52D1 (Sanz *et al.* 2005)) and PI-23472 (OR4D1 (Veitinger *et al.* 2011)); odorant mixture 3 (OM3): eugenol (OR10G7 and OR5K1 (Adipietro *et al.* 2012), OR4Q3 (Mainland *et al.* 2015)) eugenol methylether (OR51E1, OR10G7 and OR5K1 (Adipietro *et al.* 2012)), geraniol (OR2M7, OR1A1 and OR2W1 (Saito *et al.* 2009)), menthol (OR8K3, OR51E1 and OR2J2 (Adipietro *et al.* 2012)) and S-citronellal (OR1A2 (Schmiedeberg *et al.* 2007)); and odorant mixture 4 (OM4):  $\gamma$ -decalactone (OR1G1 (Sanz *et al.* 2005)) and cis-3-hexen-1-ol (OR2J2, OR2J3 and OR2W1 (McRae *et al.* 2012)). All of the odorants were kindly provided by Dr J Panten (Symrise AG, Holzminden, Germany) and were initially dissolved in DMSO.

### Serotonin release measurement

The release of serotonin was measured as described elsewhere (Doihara *et al.* 2009). QGP-1 cells were seeded

in the range  $2 \times 10^5$  cells/well in a 24-well plate. After 72 h, the medium was removed and the cells were washed in PBS containing 0.1% BSA and  $2 \mu\text{M}$  fluoxetine. Helional and 8-bromo-cGMP (prediluted in DMSO) were diluted in 0.25 mL PBS and incubated with QGP-1 cells for 20 min at  $37^\circ\text{C}$ . The assay buffer was then collected and centrifuged for 5 min at  $1000g$ . The supernatant was removed and stored at  $-80^\circ\text{C}$ . Enzyme-linked immunosorbent assay (ELISA) (Enzo Life Sciences, Farmingdale, NY, USA) was performed to measure the serotonin concentration in the supernatant according to the manufacturer's protocol.

### Statistical analysis

All the results were tested for normality and equal variance. Significant outliers were detected via GraphPad QuickCalcs (Grubb's test) (<http://graphpad.com/quickcalcs/Grubbs1.cfm>). The data that passed the equal variance and normality tests were subjected to a two-tailed unpaired *t*-test or a one-way ANOVA with post hoc test (Tukey). The data that failed the aforementioned tests were subjected to a Mann-Whitney *U* test. All values represent mean  $\pm$  standard error of the mean (s.e.m.) of at least three independent experiments. In all figures, the significance of differences is represented as follows: n.s.=not significant, \* $P < 0.05$ , \*\* $P < 0.01$  and \*\*\* $P < 0.001$ .

## Results

### Odorant mixtures elicit a transient Ca<sup>2+</sup> decrease in the QGP-1 cells

To evaluate the chemosensory properties of the QGP-1 cells, we conducted ratiofluorometric Ca<sup>2+</sup> imaging experiments. We applied four odor mixtures (OM1-4, see 'Materials and methods' section) through a custom-made air pressure-driven system. Each of the mixtures consisted of a different set of odorants, which are all known activators of ORs (see 'Materials and methods' section). Therefore, any changes observed in the intracellular Ca<sup>2+</sup> levels could indicate the specific activation of a certain OR within the QGP-1 cells.

Application of OM1 (Fig. 1A and E) or OM3 (Fig. 1C and E) initiated a transient intracellular Ca<sup>2+</sup> decrease in the QGP-1 cells (OM1:  $-0.230 \pm 0.046$ ; OM3:  $-0.172 \pm 0.029$ ), whereas neither OM2 (Fig. 1B) nor OM4 (Fig. 1D) or Ringer's solution with 0.1% DMSO affected the intracellular Ca<sup>2+</sup> concentration (Supplementary Fig. 1, see section on supplementary data given at the

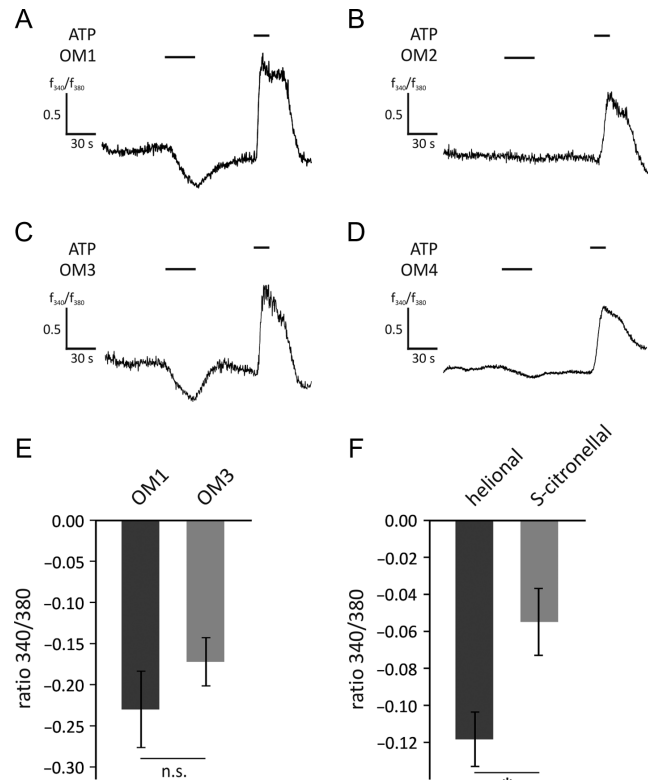


**Figure 1**

Odorant mixtures and single odorants elicited decreases in the intracellular Ca<sup>2+</sup> level in QGP-1 cells. (A–D) Sample traces of ratiometric Ca<sup>2+</sup> imaging experiments with four different odorant mixtures (OM1–4). The odorant mixtures (OM) were applied for 30 s. Each single odorant in the OM had a final concentration of  $300 \mu\text{M}$ . OM1 (A) and OM3 (C) produced strong decreases in the intracellular Ca<sup>2+</sup> during the application. (E) Bar graph of the 340 nm/380 nm ratio showing the maximal decrease in the Ca<sup>2+</sup> when OM1 ( $N=6$ ) or 3 ( $N=5$ ) was applied. (F) The single odorants helional ( $300 \mu\text{M}$ , odorant of OM1) ( $N=5$ ) and S-citronellal ( $300 \mu\text{M}$ , odorant of OM 3) ( $N=4$ ) produced visible decreases in the intracellular Ca<sup>2+</sup> level. As a viability control, ATP ( $100 \mu\text{M}$ ) was applied at the end of every measurement. The bars shown in all experimental traces indicate the durations of the stimuli. Bars are representing the mean  $\pm$  s.e.m.. The significance was tested using an unpaired two-sample Student's *t*-test. n.s.=not significant, \* $P < 0.05$ .

end of this article). The strength of the odorant-induced Ca<sup>2+</sup> decrease was dependent on the cell's basal Ca<sup>2+</sup> concentration: an example is shown for the application of OM1 (Supplementary Fig. 2). We further analyzed the Ca<sup>2+</sup> changes mediated by single odorants of the aforementioned effective mixes. Of all of the tested odorants, only helional (an agonist for OR3A1, OR1A2 and OR2J3) (Wetzel *et al.* 1999, Adipietro *et al.* 2012) and S-citronellal (OR1A1 and OR1A2) (Schmiedeberg *et al.* 2007) induced an intracellular Ca<sup>2+</sup> decrease (Fig. 1F). The decrease of the intracellular Ca<sup>2+</sup> concentration induced by helional ( $-0.118 \pm 0.015$ ) was significantly higher compared with the effect of S-citronellal ( $-0.054 \pm 0.018$ ).

Therefore, we further characterized the helional-induced effects on QGP-1 cells.

### OR2J3 is expressed in the QGP-1 cells

Previous findings identified three different ORs activated by helional. To examine whether the RNA for these ORs was present in the QGP-1 cells, we performed RT-PCR experiments using specific primers for OR2J3, OR1A2 and OR3A1. We detected transcripts for OR2J3, but not for OR1A2 and OR3A1 (Fig. 2A). Primer specificity was tested with human gDNA (Supplementary Fig. 3). In addition, we conducted Western blotting and immunocytochemical staining of the QGP-1 cells using an antibody specific for OR2J3. We showed that OR2J3 was also present at the protein level and was located at the cell membrane and in the cytoplasm (Fig. 2B and D). A primary antibody against  $\beta$ -actin was used for the loading control (Fig. 2C). A secondary antibody control sample showed no specific staining (Fig. 2E).

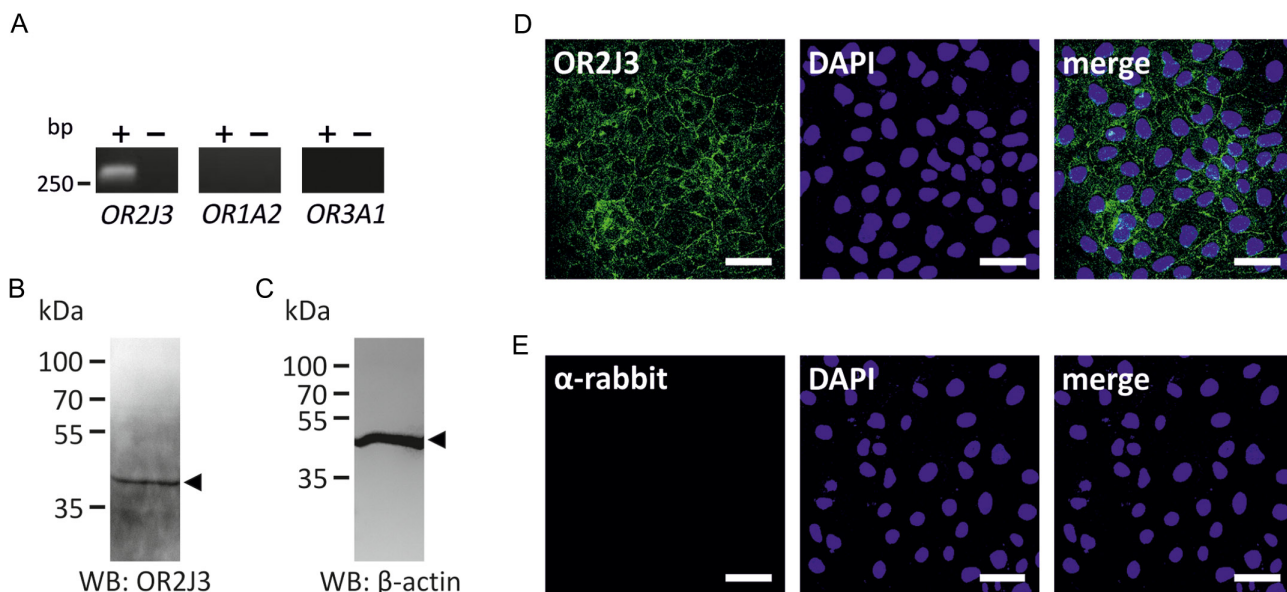
### Helional induces a dose-dependent Ca<sup>2+</sup> decrease in the QGP-1 cells

Because application of helional triggered a reduction in the Ca<sup>2+</sup> levels, we monitored this effect in more detail.

We analyzed the dose dependency of the helional-induced transient Ca<sup>2+</sup> decrease in QGP-1 cells. The application of 100, 300 or 800  $\mu$ M helional caused a dose-dependent effect, as indicated by decreases in the  $f_{340}/f_{380}$  ratio with increasing concentrations of the odorant (100  $\mu$ M:  $-0.020 \pm 0.010$ ; 300  $\mu$ M:  $-0.036 \pm 0.018$ ; 800  $\mu$ M:  $-0.063 \pm 0.022$ ) (Fig. 3A and B). Helional at 800  $\mu$ M concentration induced a significant decrease in the Ca<sup>2+</sup> concentration compared with 100  $\mu$ M and 500  $\mu$ M. Stimulation with a control odorant, 500  $\mu$ M amyl butyrate from the ineffective OM2, did not elicit any changes in the intracellular Ca<sup>2+</sup> concentration (Fig. 3A).

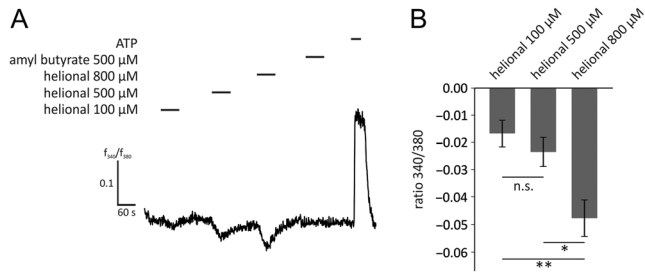
### The helional-induced Ca<sup>2+</sup> decrease in QGP-1 cells is PKG dependent

To identify the possible molecular mechanisms leading to the helional-induced Ca<sup>2+</sup> decrease in QGP-1 cells, we applied the direct activator of the protein kinase G (PKG), 8-bromo-cGMP (100  $\mu$ M), to the cells and measured the intracellular Ca<sup>2+</sup> levels using Ca<sup>2+</sup> imaging. In previous studies, it has been shown that PKG can induce a decrease in the basal Ca<sup>2+</sup> calcium levels (Zhuang 2004). After applying 100  $\mu$ M 8-bromo-cGMP to QGP-1 cells, we observed a reduction in Ca<sup>2+</sup>. The amplitude was comparable with that evoked by



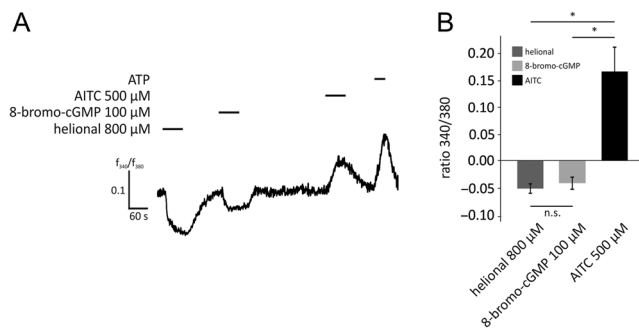
**Figure 2**

Expression of olfactory receptors (ORs) at the transcript and protein levels in QGP-1. (A) A band specific for OR2J3 (~250 bp) could be detected after qualitative PCR (qPCR) of the QGP-1 cDNA using the OR2J3-specific primers. (B and C) Western blotting analysis of the QGP-1 protein lysate incubated with an OR2J3-specific antibody revealed a single band at ~40 kDa (B). As a loading control, a  $\beta$ -actin-specific antibody was used, and a band at ~40 kDa was visible (C). (D, E) Immunocytochemical staining of the QGP-1 cells showed that OR2J3 is membrane and cytoplasm localized (D). The anti-rabbit secondary antibody control showed no specific staining (E). The cell nuclei were stained with 4'-6-diamidin-2-phenylindol (DAPI). Scale bars: 50  $\mu$ M.

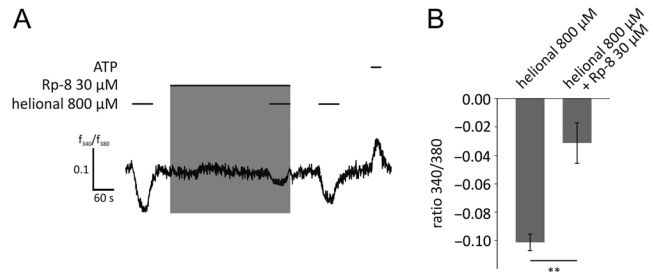
**Figure 3**

The helional-induced Ca<sup>2+</sup> decrease was dose dependent. (A) An example of a trace from a Ca<sup>2+</sup> imaging experiment with various concentrations of helional (100, 500 and 800 μM; stimulus: 60 s). Amylin butyrate (500 μM) was tested as a control stimulus and induced no visible Ca<sup>2+</sup> increase or decrease. As a viability control, ATP (100 μM) was applied at the end of every measurement. The bars indicate the stimulus duration. (B) Helional induced a significant Ca<sup>2+</sup> decrease at concentrations of 500 μM and 800 μM compared with that at 100 μM (*N*=8). Bars represent mean ± s.e.m. The significance was tested using a one-way ANOVA with post hoc test (Tukey). n.s. = not significant, \**P*<0.05, \*\**P*<0.01.

800 μM helional (8-bromo-cGMP 100 μM:  $-0.041 \pm 0.011$ ; helional 800 μM:  $-0.051 \pm 0.009$ ) (Fig. 4A and B). The expression of TRPA1 and its stimulation with AITC have been described previously in QGP-1 cells (Doihara *et al.* 2009). We therefore stimulated the cells with 500 μM AITC to confirm TRPA1 activation and observed a robust intracellular Ca<sup>2+</sup> increase ( $0.166 \pm 0.045$ ). To confirm the viability of the cells, we applied ATP at the end of every experiment, which led to an elevation of Ca<sup>2+</sup>.

**Figure 4**

8-bromo-cGMP, a protein kinase G (PKG) activator, led to a Ca<sup>2+</sup> decrease similar to the helional-evoked responses. (A) Sample trace of Ca<sup>2+</sup> imaging experiment showing the Ca<sup>2+</sup> decrease induced by helional (800 μM; stimulus: 60 s) and 8-bromo-cGMP (100 μM; stimulus: 60 s). The cells were then stimulated with AITC (500 μM; stimulus: 60 s) to activate the TRPA1-mediated Ca<sup>2+</sup> increase. As a viability control, ATP (100 μM) was applied at the end of every measurement. The bars indicate the stimulus duration. (B) Bar graph showing the Ca<sup>2+</sup> decreases induced by helional and 8-bromo-cGMP. In contrast, AITC led to a significant increase in the intracellular Ca<sup>2+</sup> (*N*=6). Bars represent mean ± s.e.m. The significance was tested using a one-way ANOVA with post hoc test (Tukey). n.s. = not significant, \**P*<0.05.

**Figure 5**

Co-application of the PKG-specific blocker Rp-8-pCPT-cGMPs (Rp-8) led to a significant inhibition of the helional-induced Ca<sup>2+</sup> decrease. (A) Sample trace of a ratiometric Ca<sup>2+</sup>-imaging experiment. First, helional (800 μM) was applied for 60 s. Rp-8 (30 μM) was then added for 6 min before the co-application of helional (800 μM; stimulus: 60 s). After 60 s of washing with extracellular solution, helional (800 μM; stimulus: 60 s) was applied again. As a viability control, ATP (100 μM) was applied at the end of every measurement. The bars indicate the stimulus duration. (B) Rp-8 (30 μM) caused a significant inhibition of the helional (800 μM)-evoked Ca<sup>2+</sup> decrease (*N*=6). Bars represent mean ± s.e.m. The significance was tested using an unpaired two-sample Student's *t*-test. \*\**P*<0.01.

Furthermore, we tested the specific PKG blocker, Rp-8-pCPT-cGMPs (Rp-8) (50 μM), in combination with 800 μM helional on QGP-1 cells. The inhibition of PKG led to a significant suppression of the helional-dependent Ca<sup>2+</sup> decrease (helional:  $-0.101 \pm 0.006$ ; helional+Rp-8:  $-0.031 \pm 0.014$ ), thus confirming the involvement of PKG in the helional-induced signaling (Fig. 5A and B).

### Helional initiates a dose-dependent release of serotonin from QGP-1 cells

Next, we were interested in the physiological relevance of the helional-induced Ca<sup>2+</sup> decrease in QGP-1 cells. In previous studies, it was reported that QGP-1 cells release serotonin upon TRPA1 activation (Doihara *et al.* 2009, Schulze *et al.* 2013). We therefore used a serotonin-specific ELISA kit to determine whether OR activation affected the serotonin release by measuring the serotonin concentration after the stimulation of QGP-1 cells with various concentrations of helional (10, 300, 800 and 1000 μM) or with 8-bromo-cGMP for 15 min. The application of helional led to a dose-dependent increase in the serotonin secretion (Fig. 6) (0.1% DMSO:  $2.715 \pm 0.12$  ng/mL; 10 μM:  $2.901 \pm 0.188$  ng/mL; 300 μM:  $4.102 \pm 0.229$  ng/mL; 800 μM:  $10.028 \pm 0.775$  ng/mL; 1000 μM:  $12.658 \pm 1.039$  ng/mL). Additionally, stimulation with the PKG activator 8-bromo-cGMP caused a similar release of serotonin ( $4.997 \pm 0.652$  ng/mL), which was significantly different from the DMSO (0.1%) control.

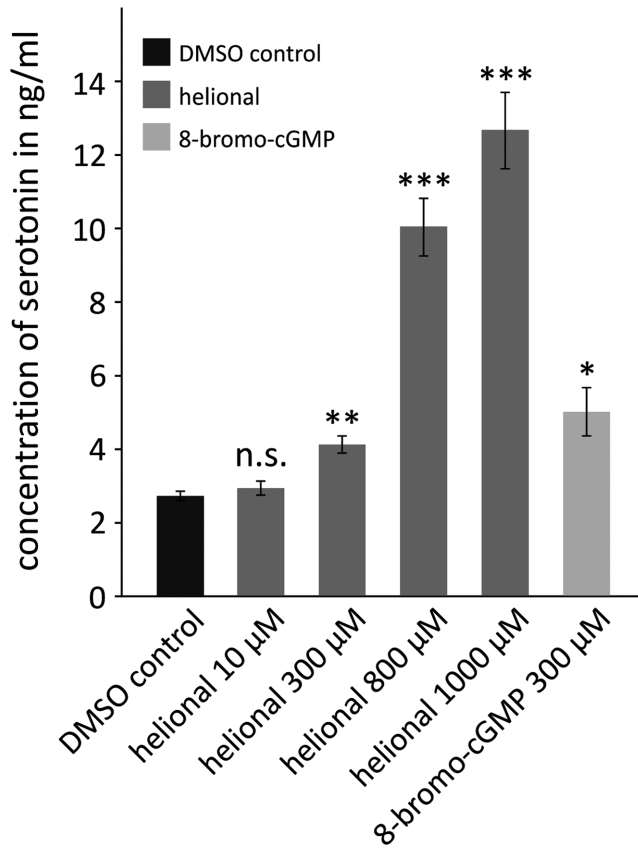


**Figure 6**

Stimulation of QGP-1 cells with helional 10 µM ( $N=6$ ), 300 µM ( $N=6$ ), 800 µM ( $N=6$ ) and 1000 µM ( $N=6$ ) led to an increase in the extracellular serotonin concentration in ng/mL. The cells were stimulated for 15 min, and the extracellular serotonin concentration was measured using a commercially available ELISA kit. The obvious increase in the secretion of serotonin induced by helional was concentration dependent and was significant at a concentration of 300 µM compared with the DMSO (0.1%) control ( $N=3$ ). The PKG activator 8-bromo-cGMP (300 µM) ( $N=3$ ) also produced a significant increase in the serotonin concentration compared with the DMSO control. Bars represent mean  $\pm$  S.E.M. The significance was tested using an unpaired two-sample Student's  $t$ -test. \* $P < 0.05$ , \*\* $P < 0.01$ , \*\*\* $P < 0.001$ .

## Discussion

In the last decade, human ORs have been identified in various nonchemosensory cell types and tissues outside the nose (Feldmesser *et al.* 2006, Flegel *et al.* 2013); however, only a few physiological studies have been carried out at present (Spehr *et al.* 2003, Neuhaus *et al.* 2009, Busse *et al.* 2014, Maßberg *et al.* 2015, Manteniots *et al.* 2016).

We present the first data that show that OR2J3 is expressed at the mRNA level in the human pancreatic neuroendocrine tumor cell line QGP-1. We confirmed the presence of OR2J3 at the protein level via Western blotting

analysis and immunocytochemical experiments with an OR2J3-specific antibody and saw a specific OR staining in the membrane and the cytoplasm of the cells. The expression of other ORs (hOR73, hOR17-7/11, hOR1G1 and hOR17-210) has already been reported for the human EC BON cell line (Braun *et al.* 2007). In addition, TRPA1 has been identified in QGP-1 cells (Doihara *et al.* 2009). Both ORs and TRP channels trigger an intracellular Ca<sup>2+</sup> increase followed by a release of serotonin (Braun *et al.* 2007, Doihara *et al.* 2009). Remarkably, we found that the application of four different odorant mixtures and the single odorant helional, which activates OR2J3 and OR3A1 (Wetzel *et al.* 1999, Jacquier *et al.* 2006), led to a transient concentration-dependent Ca<sup>2+</sup> decrease in QGP-1 cells. Odorant-dependent intracellular Ca<sup>2+</sup> decreases have been demonstrated previously for feline (Gomez *et al.* 2005), human (Rawson *et al.* 1997, Gomez *et al.* 2000) and mudpuppy (Delay 2002) OSNs, showing that distinct ORs initiate not only the canonical Ca<sup>2+</sup> increases but also decreases within the olfactory system. Furthermore, it is already known that  $\alpha_{1D}$ -adrenoceptors are able to modulate the Ca<sup>2+</sup> levels in fibroblasts that lead to decreases in the basal Ca<sup>2+</sup> level (García-Sáinz & Torres-Padilla 1999). However, the molecular identity of the underlying signal transduction pathway currently remains unresolved. We therefore aimed to elucidate the possible signaling components involved in this process. As we observed only decreases in the intracellular Ca<sup>2+</sup>, we did not further concentrate on classical olfactory signaling proteins, such as the adenylyl cyclase III (Lowe *et al.* 1989, Bakalyar & Reed 1990), or the cyclic nucleotide-gated Ca<sup>2+</sup> channel (Nakamura & Gold 1987), which have been investigated in detail by other studies that used ectopically expressed ORs (Busse *et al.* 2014, Maßberg *et al.* 2015, Manteniots *et al.* 2016). Previous studies have shown that the activation of other alternative olfactory signaling molecules, such as phospholipase C or Src kinases, causes increases in the Ca<sup>2+</sup> levels or inhibits the odorant-induced Ca<sup>2+</sup> increases (Spehr *et al.* 2002, Ache 2010). We therefore did not analyze those in the QGP-1 cells. Importantly, it has been shown that the cyclic guanosine monophosphate (cGMP)-dependent protein kinase (PKG) regulates the vascular reactivity and tone in smooth muscle cells through a reduction of the intracellular Ca<sup>2+</sup> levels (Taylor *et al.* 2004). Furthermore, PKG-mediated pathways can inhibit the opening of the TRP and N-type Ca<sup>2+</sup> channels and modulate the L-type Ca<sup>2+</sup> channels in neuroblastoma cells, cardiomyocytes and atrial cells (Wang *et al.* 2000, D'Ascenzo *et al.* 2002, Koitabashi *et al.* 2010). Previous studies have demonstrated that the activation

of PKG directly phosphorylates TRPC3 and TRPC6 and thereby decreases the influx of Ca<sup>2+</sup> (Kwan *et al.* 2004, Koitabashi *et al.* 2010). Thus, we applied the known PKG activator 8-bromo-cGMP to the QGP-1 cells and observed a Ca<sup>2+</sup> decrease comparable with the helional-dependent response. In addition, treatment with the PKG-specific blocker Rp-8-pCPT-cGMPS significantly inhibited the odorant-dependent Ca<sup>2+</sup> decrease, thus proving that PKG was involved in the helional-induced signaling pathway. However, the detailed pathway remains elusive. It is possible that constitutively open channels might be inhibited through the activation of PKG, which would then lead to a decrease in the basal Ca<sup>2+</sup> level. Potential targets might be the TRP channels (for example TRPA1, TRPV5 and TRPV6), which are known to be constitutively open (Nilius 2007).

We found that the application of helional led to a release of serotonin in a dose-dependent manner, thus demonstrating the physiological relevance of this newly identified signaling cascade. Previous studies demonstrated that serotonin release from EC cells by odorants is coupled to an increase in intracellular Ca<sup>2+</sup> (Kim *et al.* 2001, Braun *et al.* 2007, Doihara *et al.* 2009). In contrast, we showed that beside the Ca<sup>2+</sup> reduction, helional led to an increase in serotonin release. We suggest that a Ca<sup>2+</sup>-independent pathway might lead to an increase of the serotonin release based on a so far unknown mechanism. One study showed that insulin exocytosis is independent of the intracellular Ca<sup>2+</sup> increase or membrane depolarization in pancreatic B cells (Lang *et al.* 1998). Therefore, GPCR-mediated processes can directly lead to exocytosis without ion flux. Furthermore, we showed that 8-bromo-cGMP, the activator of PKG, led to a comparable increase in the release of serotonin. In the EC cell line BON, the vesicular release of  $\gamma$ -aminobutyric acid (GABA) and chromogranin A is mediated by cGMP and is therefore independent of the Ca<sup>2+</sup> level (John *et al.* 1998). We suggest that serotonin release can also be mediated by the activation of PKG in QGP-1 cells. The GPCR-mediated phosphorylation of mitogen-activated protein kinase (MAPK) ERK leads to the secretion of serotonin in EC cells (Kidd *et al.* 2008, Chin *et al.* 2012). In platelets, the phosphorylation of ERK is dependent on a cGMP/PKG signaling pathway (Li *et al.* 2006). A similar pathway in QGP-1 cells upon activation with helional seems to be conceivable. Furthermore, there might be currently uncharacterized signaling components involved in the release of serotonin. This has to be investigated in further studies.

In summary, we described an odorant-activated signaling pathway in human QGP-1 cells that triggered the release of serotonin and led to a decrease in Ca<sup>2+</sup> induced by PKG. Thus, this study provides important information that will lead to a better understanding of the activating mechanisms for EC cells and the symptoms of several diseases associated with these cells, including irritable bowel syndrome. These results also emphasize the ORs as novel putative clinical targets. For the first time, we showed that the ORs are able to reduce the intracellular Ca<sup>2+</sup> concentration in nonolfactory cells. Our study therefore describes the novel discovery of an OR-related signaling to an odorant stimulus in EC cells.

#### Supplementary data

This is linked to the online version of the paper at <http://dx.doi.org/10.1530/JME-16-0063>.

#### Declaration of interest

The authors declare that there is no conflict of interest that could be perceived as prejudicing the impartiality of the research reported.

#### Funding

This research project was financially supported by the Deutsche Forschungsgemeinschaft grant numbers SFB 874 and SFB 642 and the Ruhr-University Research School.

#### Author contribution statement

B K, H H and S O helped in conception and design; B K, M S, J M, P S, F J and S O carried out the analysis and interpretation; B K, H H and S O drafted the manuscript for important intellectual content.

#### Acknowledgements

QGP-1 cells were kindly provided by Prof Dr Massimo Donadelli (University of Verona, Italy). The authors thank Dr Günter Gisselmann for his support regarding molecular biological techniques and Simon Pyschny for the technical support.

#### References

- Ache BW 2010 Odorant-specific modes of signaling in mammalian olfaction. *Chemical Senses* **35** 533–539. (doi:10.1093/chemse/bjq045)
- Adipietro KA, Mainland JD & Matsunami H 2012 Functional evolution of mammalian odorant receptors. *PLoS Genetics* **8** e1002821. (doi:10.1371/journal.pgen.1002821)
- Bakalyar HA & Reed RR 1990 Identification of a specialized adenylyl cyclase that may mediate odorant detection. *Science* **250** 1403–1406. (doi:10.1126/science.2255909)
- Bischoff SC, Barbara G, Buurman W, Ockhuizen T, Schulzke J-D, Serino M, Tilg H, Watson A & Wells JM 2014 Intestinal permeability – a new



- target for disease prevention and therapy. *BMC Gastroenterology* **14** 189. (doi:10.1186/s12876-014-0189-7)
- Braun T, Volland P, Kunz L, Prinz C & Gratzl M 2007 Enterochromaffin cells of the human gut: sensors for spices and odorants. *Gastroenterology* **132** 1890–1901. (doi:10.1053/j.gastro.2007.02.036)
- Busse D, Kudella P, Grüning N-M, Gisselmann G, Ständer S, Luger T, Jacobsen F, Steinsträßer L, Paus R, Gkogkolou P, et al. 2014 A synthetic sandalwood odorant induces wound-healing processes in human keratinocytes via the olfactory receptor OR2AT4. *Journal of Investigative Dermatology* **134** 2823–2832. (doi:10.1038/jid.2014.273)
- Chin A, Svejda B, Gustafsson BI, Granlund AB, Sandvik AK, Timberlake A, Sumpio BE, Pfragner R, Modlin IM & Kidd M 2012 The role of mechanical forces and adenosine in the regulation of intestinal enterochromaffin cell serotonin secretion. *American Journal of Physiology: Gastrointestinal and Liver Physiology* **302** G397–G405. (doi:10.1152/ajpgi.00087.2011)
- D'Ascenzo M, Martinotti G, Azzena GB & Grassi C 2002 cGMP/protein kinase G-dependent inhibition of N-type Ca<sup>2+</sup> channels induced by nitric oxide in human neuroblastoma IMR32 cells. *Journal of Neuroscience* **22** 7485–7492.
- Delay RJ 2002 Two second messengers mediate amino acid responses in olfactory sensory neurons of the salamander, *Neoturus maculosus*. *Chemical Senses* **27** 673–680. (doi:10.1093/chemse/27.8.673)
- Doihara H, Nozawa K, Kojima R, Kawabata-Shoda E, Yokoyama T & Ito H 2009 QGP-1 cells release 5-HT via TRPA1 activation; a model of human enterochromaffin cells. *Molecular and Cellular Biochemistry* **331** 239–245. (doi:10.1007/s11010-009-0165-7)
- Feldmesser E, Olender T, Khen M, Yanai I, Ophir R & Lancet D 2006 Widespread ectopic expression of olfactory receptor genes. *BMC Genomics* **7** 121. (doi:10.1186/1471-2164-7-121)
- Flegel C, Manteniotis S, Osthold S, Hatt H & Gisselmann G 2013 Expression profile of ectopic olfactory receptors determined by deep sequencing. *PLoS ONE* **8** e55368. (doi:10.1371/journal.pone.0055368)
- García-Sáinz JA & Torres-Padilla ME 1999 Modulation of basal intracellular calcium by inverse agonists and phorbol myristate acetate in rat-1 fibroblasts stably expressing  $\alpha(1d)$ -adrenoceptors. *FEBS Letters* **443** 277–281. (doi:10.1016/S0014-5793(98)01738-4)
- Gershon MD 2004 Review article: serotonin receptors and transporters – roles in normal and abnormal gastrointestinal motility. *Alimentary Pharmacology & Therapeutics* **20** (Supplement 7) 3–14. (doi:10.1111/j.1365-2036.2004.02180.x)
- Gershon MD 2013 5-Hydroxytryptamine (serotonin) in the gastrointestinal tract. *Current Opinion in Endocrinology, Diabetes Obesity* **20** 14–21. (doi:10.1097/MED.0b013e32835bc703)
- Gomez G, Rawson NE, Cowart B, Lowry LD, Pribitkin EA & Restrepo D 2000 Modulation of odor-induced increases in [Ca<sup>2+</sup>]<sub>i</sub> by inhibitors of protein kinases A and C in rat and human olfactory receptor neurons. *Neuroscience* **98** 181–189. (doi:10.1016/S0306-4522(00)00112-3)
- Gomez G, Lischka FW, Haskins ME & Rawson NE 2005 Evidence for multiple calcium response mechanisms in mammalian olfactory receptor neurons. *Chemical Senses* **30** 317–326. (doi:10.1093/chemse/bji026)
- Heredia DJ, Gershon MD, Koh SD, Corrigan RD, Okamoto T & Smith TK 2013 Important role of mucosal serotonin in colonic propulsion and peristaltic reflexes: in vitro analyses in mice lacking tryptophan hydroxylase 1. *Journal of Physiology* **591** 5939–5957. (doi:10.1113/jphysiol.2013.256230)
- Iguchi H, Hayashi I & Kono A 1990 A somatostatin-secreting cell line established from a human pancreatic islet cell carcinoma (somatostatinoma): release experiment and immunohistochemical study. *Cancer Research* **50** 3691–3693.
- Jacquier V, Pick H & Vogel H 2006 Characterization of an extended receptive ligand repertoire of the human olfactory receptor OR17-40 comprising structurally related compounds. *Journal of Neurochemistry* **97** 537–544. (doi:10.1111/j.1471-4159.2006.03771.x)
- John M, Wiedenmann B, Kruhoffer M, Adermann K, Ankorina-Stark I, Schlatter E, Ahnert-Hilger G, Forssmann WG & Kuhn M 1998 Guanylin stimulates regulated secretion from human neuroendocrine pancreatic cells. *Gastroenterology* **114** 791–797. (doi:10.1016/S0016-5085(98)70593-1)
- Kidd M, Modlin IM, Gustafsson BI, Drozdov I, Hauso O & Pfragner R 2008 Luminal regulation of normal and neoplastic human EC cell serotonin release is mediated by bile salts, amines, tastants, and olfactants. *American Journal of Physiology: Gastrointestinal and Liver Physiology* **295** G260–G272. (doi:10.1152/ajpgi.00056.2008)
- Kim M, Cooke HJ, Javed NH, Carey H V, Christofi F & Raybould HE 2001 D-glucose releases 5-hydroxytryptamine from human BON cells as a model of enterochromaffin cells. *Gastroenterology* **121** 1400–1406. (doi:10.1053/gast.2001.29567)
- Koitaishi N, Aiba T, Hesketh GG, Rowell J, Zhang M, Takimoto E, Tomaselli GF & Kass DA 2010 Cyclic GMP/PKG-dependent inhibition of TRPC6 channel activity and expression negatively regulates cardiomyocyte NFAT activation. *Journal of Molecular and Cellular Cardiology* **48** 713–724. (doi:10.1016/j.yjmcc.2009.11.015)
- Kwan HY, Huang Y & Yao X 2004 Regulation of canonical transient receptor potential isoform 3 (TRPC3) channel by protein kinase G. *PNAS* **101** 2625–2630. (doi:10.1073/pnas.0304471101)
- Lang J, Ushkaryov Y, Grasso A & Wollheim CB 1998 Ca<sup>2+</sup>-independent insulin exocytosis induced by  $\alpha$ -latrotoxin requires latrophilin, a G protein-coupled receptor. *EMBO Journal* **17** 648–657. (doi:10.1093/emboj/17.3.648)
- Li Z, Zhang G, Feil R, Han J & Du X 2006 Sequential activation of p38 and ERK pathways by cGMP-dependent protein kinase leading to activation of the platelet integrin  $\alpha$  IIb $\beta$ 3. *Blood* **107** 965–972. (doi:10.1182/blood-2005-03-1308)
- Li Z, Chalazonitis A, Huang Y-Y, Mann JJ, Margolis KG, Yang QM, Kim DO, Côté F, Mallet J & Gershon MD 2011 Essential roles of enteric neuronal serotonin in gastrointestinal motility and the development/survival of enteric dopaminergic neurons. *Journal of Neuroscience* **31** 8998–9009. (doi:10.1523/JNEUROSCI.6684-10.2011)
- Lowe G, Nakamura T & Gold GH 1989 Adenylate cyclase mediates olfactory transduction for a wide variety of odorants. *PNAS* **86** 5641–5645. (doi:10.1073/pnas.86.14.5641)
- Mainland JD, Li YR, Zhou T, Liu WLL & Matsunami H 2015 Human olfactory receptor responses to odorants. *Scientific Data* **2** 150002. (doi:10.1038/sdata.2015.2)
- Manocha M & Khan WI 2012 Serotonin and GI disorders: an update on clinical and experimental studies. *Clinical and Translational Gastroenterology* **3** e13. (doi:10.1038/ctg.2012.8)
- Manteniotis S, Wojcik S, Brauhoff P, Möllmann M, Petersen L, Göthert J, Schmiel W, Dührsen U, Gisselmann G & Hatt H 2016 Functional characterization of the ectopically expressed olfactory receptor 2AT4 in human myelogenous leukemia. *Cell Death Discovery* **2** 15070. (doi:10.1038/cddiscovery.2015.70)
- Maßberg D, Simon A, Häussinger D, Keitel V, Gisselmann G, Conrad H & Hatt H 2015 Monoterpene (-)-citronellal affects hepatocarcinoma cell signaling via an olfactory receptor. *Archives of Biochemistry and Biophysics* **566** 100–109. (doi:10.1016/j.abb.2014.12.004)
- McRae JF, Mainland JD, Jaeger SR, Adipietro KA, Matsunami H & Newcomb RD 2012 Genetic variation in the odorant receptor OR2J3 is associated with the ability to detect the 'grassy' smelling odor, cis-3-hexen-1-ol. *Chemical Senses* **37** 585–593. (doi:10.1093/chemse/bjs049)
- Moran GW, Leslie FC, Levison SE & McLaughlin JT 2008 Review: enteroendocrine cells: neglected players in gastrointestinal disorders? *Therapeutic Advances in Gastroenterology* **1** 51–60. (doi:10.1177/1756283X08093943)
- Nakamura T & Gold GH 1987 A cyclic nucleotide-gated conductance in olfactory receptor cilia. *Nature* **325** 443–444. (doi:10.1038/325442a0)
- Neuhaus EM, Mashukova A, Zhang W, Barbour J & Hatt H 2006 A specific heat shock protein enhances the expression of mammalian

- olfactory receptor proteins. *Chemical Senses* **31** 445–452. (doi:10.1093/chemse/bjj049)
- Neuhaus EM, Zhang W, Gelis L, Deng Y, Noldus J & Hatt H 2009 Activation of an olfactory receptor inhibits proliferation of prostate cancer cells. *Journal of Biological Chemistry* **284** 16218–16225. (doi:10.1074/jbc.M109.012096)
- Nilius B 2007 TRP channels in disease. *Biochimica et Biophysica Acta* **1772** 805–812. (doi:10.1016/j.bbadis.2007.02.002)
- Pavlati GK 2010 A new function for odorant receptors: MOR23 is necessary for normal tissue repair in skeletal muscle. *Cell Adhesion and Migration* **4** 502–506. (doi:10.4161/cam.4.4.12291)
- Pfragner R, Behmel A, Höger H, Beham A, Ingolic E, Stelzer I, Svejda B, Moser VA, Obenauf AC, Siegl V, *et al.* 2009 Establishment and characterization of three novel cell lines – P-STS, L-STS, H-STS – derived from a human metastatic midgut carcinoid. *Anticancer Research* **29** 1951–1961.
- Racké K, Reimann A, Schwörer H & Kilbinger H 1996 Regulation of 5-HT release from enterochromaffin cells. *Behavioural Brain Research* **73** 83–87. (doi:10.1016/0166-4328(96)00075-7)
- Rawson NE, Gomez G, Cowart B, Brand JG, Lowry LD, Pribitkin EA & Restrepo D 1997 Selectivity and response characteristics of human olfactory neurons. *Journal of Neurophysiology* **77** 1606–1613.
- Saito H, Chi Q, Zhuang H, Matsunami H & Mainland JD 2009 Odor coding by a mammalian receptor repertoire. *Science Signaling* **2** ra9. (doi:10.1126/scisignal.2000016)
- Sanz G, Schlegel C, Pernollet J-C & Briand L 2005 Comparison of odorant specificity of two human olfactory receptors from different phylogenetic classes and evidence for antagonism. *Chemical Senses* **30** 69–80. (doi:10.1093/chemse/bji002)
- Schmiedeberg K, Shirokova E, Weber HP, Schilling B, Meyerhof W & Krautwurst D 2007 Structural determinants of odorant recognition by the human olfactory receptors OR1A1 and OR1A2. *Journal of Structural Biology* **159** 400–412. (doi:10.1016/j.jsb.2007.04.013)
- Schulze A, Oehler B, Urban N, Schaefer M & Hill K 2013 Apomorphine is a bimodal modulator of TRPA1 channels. *Molecular Pharmacology* **83** 542–551. (doi:10.1124/mol.112.081976)
- Siddique ZL, Drozdov I, Floch J, Gustafsson BI, Stunes K, Pfragner R, Kidd M & Modlin IM 2009 KRJ-I and bon cell lines: defining an appropriate enterochromaffin cell neuroendocrine tumor model. *Neuroendocrinology* **89** 458–470. (doi:10.1159/000209330)
- Spehr M, Wetzel CH, Hatt H & Ache BW 2002 3-Phosphoinositides modulate cyclic nucleotide signaling in olfactory receptor neurons. *Neuron* **33** 731–739. (doi:10.1016/S0896-6273(02)00610-4)
- Spehr M, Gisselmann G, Poplawski A, Riffell JA, Wetzel CH, Zimmer RK & Hatt H 2003 Identification of a testicular odorant receptor mediating human sperm chemotaxis. *Science* **299** 2054–2058. (doi:10.1126/science.1080376)
- Spehr J, Gelis L, Osterloh M, Oberland S, Hatt H, Spehr M & Neuhaus EM 2011 G protein-coupled receptor signaling via Src kinase induces endogenous human transient receptor potential vanilloid type 6 (TRPV6) channel activation. *Journal of Biological Chemistry* **286** 13184–13192. (doi:10.1074/jbc.M110.183525)
- Taylor MS, Okwuchukwasanya C, Nickl CK, Tegge W, Brayden JE & Dostmann WRG 2004 Inhibition of cGMP-dependent protein kinase by the cell-permeable peptide DT-2 reveals a novel mechanism of vasoregulation. *Molecular Pharmacology* **65** 1111–1119. (doi:10.1124/mol.65.5.1111)
- Veitinger T, Riffell JR, Veitinger S, Nascimento JM, Triller A, Chandsawangbhuwana C, Schwane K, Geerts A, Wunder F, Berns MW, *et al.* 2011 Chemosensory Ca<sup>2+</sup> dynamics correlate with diverse behavioral phenotypes in human sperm. *Journal of Biological Chemistry* **286** 17311–17325. (doi:10.1074/jbc.M110.211524)
- Wang YG, Wagner MB, Joyner RW & Kumar R 2000 cGMP-dependent protein kinase mediates stimulation of L-type calcium current by cGMP in rabbit atrial cells. *Cardiovascular Research* **48** 310–322. (doi:10.1016/S0008-6363(00)00178-4)
- Wetzel CH, Oles M, Wellerdieck C, Kuczkowiak M, Gisselmann G & Hatt H 1999 Specificity and sensitivity of a human olfactory receptor functionally expressed in human embryonic kidney 293 cells and *Xenopus laevis* oocytes. *Journal of Neuroscience* **19** 7426–7433.
- Wu SV, Rozengurt N, Yang M, Young SH, Sinnett-Smith J & Rozengurt E 2002 Expression of bitter taste receptors of the T2R family in the gastrointestinal tract and enteroendocrine STC-1 cells. *PNAS* **99** 2392–2397. (doi:10.1073/pnas.042617699)
- Zhuang D 2004 Essential role of protein kinase G and decreased cytoplasmic Ca<sup>2+</sup> levels in NO-induced inhibition of rat aortic smooth muscle cell motility. *American Journal of Physiology: Heart and Circulatory Physiology* **288** H1859–H1866. (doi:10.1152/ajpheart.01031.2004)

Received in final form 1 August 2016

Accepted 22 August 2016

Accepted Preprint published online 22 August 2016